HIGH INTENSITY BEAM ANALYSIS FOR THE SUPERCONDUCTING RADIO-FREQUENCY LINAC (SRF-LINAC) OF THE IFMIF-EVEDA ACCELERATORS

Wilson Simeoni Jr.*, P.A.P. Nghiem, N. Chauvin, D. Uriot
CEA/DSM/IRFU, 91191 Gif-sur-Yvette Cedex, France

Abstract

In this proceeding we analyze space-charge effects on the beam dynamics of IFMIF accelerators. The objective is to be able to characterize and understand the crucial issues like halo formation, emittance growth and sudden particle losses in the SRF-Linac. We use the Hofmann stability charts to identify modes of collective space-charge density oscillations that are responsible for the transfer and growth of the emittance. With identification of modes we are able to treat the parametric resonance between the modes and the nonlinear motion of an individual ion the amplitude of which is greater than the core radius. The resulting phase space consists of an inner separatrix containing the core and an outer separatrix that becomes the locus near which the halo particles enter and cluster.

INTRODUCTION

The IFMIF project (International Fusion Materials Irradiation Facility), aims at studying materials which must resist to very intense neutron radiations in future fusion reactors. The objective is to construct the world most intense neutron source capable of producing 10^{17} *neutrons/s* at 14 *MeV*. A major system of this project is its two accelerators producing each of them 125 *mA*. Deuteron particles up to 40 *MeV* interact with Lithium target. In a first phase called EVEDA (Engineering Validation and Engineering Design Activity), a full scale prototype accelerating particles up to 9 *MeV* is being studied and constructed in Europe, to be installed in Japan [1].

In each of the two IFMIF accelerators, D^+ particles are first accelerated by the source extraction system, then by the long Radio-Frequency Quadrupole (RFQ) and finally the Superconducting Radio-Frequency Linac (SRF-Linac) composed of four cryomodules. The first cryomodule contains 8 periods of 1 solenoid and 1 resonator ($\beta = 0.094$). The second cryomodule contains 5 periods of 1 solenoid and 2 resonators ($\beta = 0.094$). The last two cryomodules contain 4 periods of 1 solenoid and 3 resonators ($\beta = 0.166$). The total length of four cryomodules is about 22.5 *m*. At low energy, the synchronous phase starts at $-50°$ and then grows linearly with beam energy up to $-30°$. Given the beam intensity of 125 *mA*, the maximum RF power per cavity is 75 *kW* for the low-β resonators and 150 *kW* for the high-β resonators. A gradient of 4.5 *MV/m* and apertures in the $40-50$ *mm* range were chosen for the superconducting resonators. Two Half-Wave-Resonator families, with different geometric β- values, are enough to cover the acceleration from the RFQ exit (5 *MeV*) to the final energy (40 *MeV*). The axial field of the superconducting solenoid is kept around 6 *T* in order to use the classical NbTi technology for the coils [1].

In the space-charge dominated regime, the space-charge effects result in emittance growth and halo formation, which contribute to beam losses. As nonlinear space-charge forces couple the longitudinal and transverse directions, it may cause emittance exchange among different degrees of freedom if some internal resonance conditions are satisfied [2]. The main resonance band in this context is the fourth order difference resonance, which occurs in the vicinity of equal longitudinal and transverse focusing strengths. A change of focusing lattice or inadequate knowledge of proper injection conditions can cause a mismatch between the beam and the transport system. This mismatch may result in an oscillation of the beam envelope and generally excite a superposition of the envelope eigenmodes. These envelope modes possess additional free energy compared with the stationary distribution. Particles with appropriate oscillation frequencies can resonate with these envelope modes through the so called parametric $2:1$ resonance and attain large amplitude to form a halo [3]. These halo particles extract the energy from the envelope modes and convert free energy from mismatch into thermal energy, which causes beam emittance growth. The goal of this proceeding is to identify these resonances that are responsible for the coupling and growth of the emittance on the IFMIF SRF-Linac.

SPACE-CHARGE RESONANCES ON THE IFMIF SRF-LINAC

To explore the sensitivity of the IFMIF SRF-Linac design to space charge resonances, numerical simulations have been performed with TraceWin [4]. The beam distribution taken as input is the output beam from the Medium Energy Beam Transport (MEBT) , composed of more than 10^6 macroparticles. See Fig 1.

In Fig. 2 we plot the tune footprint on the Hofmann charts for the nominal emittance ratio $\epsilon_z/\epsilon_x = 1.5$ [5]. The characteristic regions of the chart indicate where the collective space charge density oscillations are expected to cause emittance transfer and growth. It is noteworthy that the unstable regions of these modes merge into the single-particle resonance conditions of difference resonances: $\nu_z - 2\nu_x \approx 0$ and $2\nu_z - \nu_x \approx 0$ for the third order even and odd modes; and $2\nu_z - 2\nu_x \approx 0$ and $\nu_z - 3\nu_x \approx 0$,

* wilson.simeoni@cea.fr

ISBN 978-3-95450-115-1

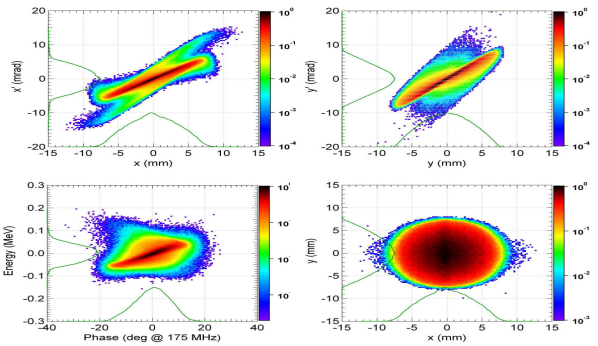

Figure 1: Beam density distribution at the IFMIF SRF-Linac entrance.

as well as $3\nu_z - \nu_x \approx 0$, for the fourth order even and odd modes. Note that a important peak is associated with the *4th*-order coupling resonance $2\nu_z - 2\nu_x \approx 0$. Two peaks at $\nu_z - 3\nu_x \approx 0$ and $\nu_z - 2\nu_x \approx 0$ have an addition direct effect on emittance transfer and growth. It should be noted that much stronger transverse tune depression (below 0.3) removes the isolated stop bands, and emittance coupling results for all tune ratios, with the exception of very small tune depression $(0.2, ..., 0.1)$, where the beam becomes increasingly equipartitioned anyway [2]. The tune footprint of IFMIF SRF-Linac reference design (red line) varies over a large interval: it intercepts the resonances $2\nu_z - 2\nu_x \approx 0$, $\nu_z - 2\nu_x \approx 0$ and $\nu_z - 3\nu_x \approx 0$. Also note that a part of tune footprint overlaps with the region (tune depression below 0.3) where resonances form a continuum, which Ingo Hofmann called the "sea of instability" [2].

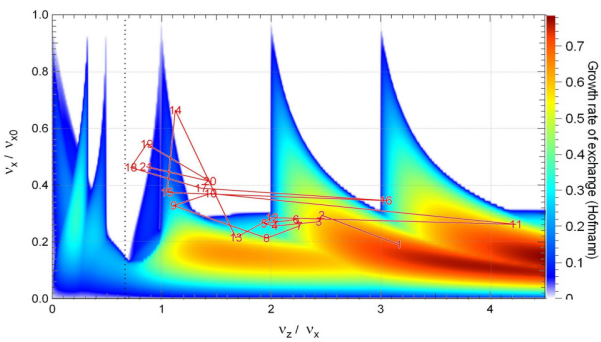

Figure 2: Stability chart for the nominal IFMIF SRF-Linac emittance ratio $\epsilon_z/\epsilon_x = 1.5$. Dashed line indicate equipartition tune ratio.

The normalized emittance variation is shown in Fig. 3. The graph shows the emittance coupling between the longitudinal and the transverse planes. The longitudinal emittance change is more pronounced than the changes of the transverse ones, since there is one "hot" plane, the longitudinal one, which is fed by the two "cold" transverse planes. In other words, the energy associated with the longitudinal plane is shared by both transverse degrees of freedom. For this reason the rms emittance evolution in the longitudinal plane has larger oscillations than those of the transverse planes. The growth of the rms emittance is analyzed by the ratio of emittance to initial emittance, see Fig 3. Since the emittance growth is a strong function of the mismatch the typical $2 : 1$ parametric resonance must be found in the phase space [3]. Numerical simulations confirm the "peanut-shape" [3] in the phase space, showing the dominant behaviour of the parametric resonance, see Fig 4. In Fig. 4 only halo particles are plotted. The halo part of the beam is defined as the part outside the position where the second derivative of the beam density profile is maximum [6].

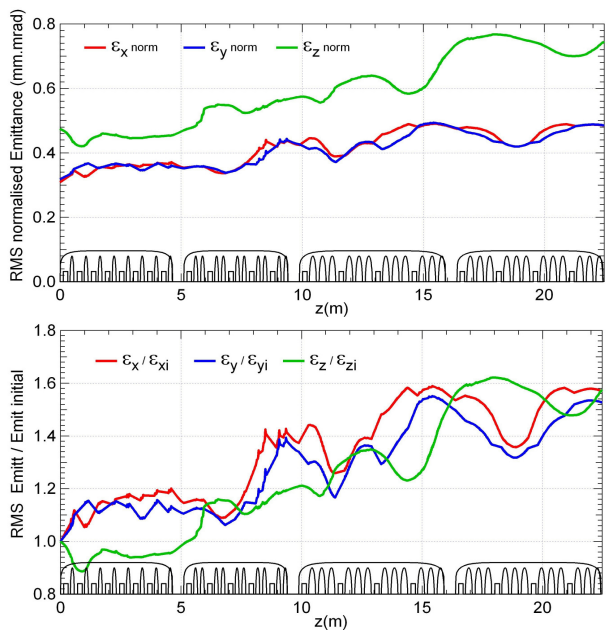

Figure 3: Above : normalised emittance along the IFMIF SRF-Linac. Below : ratio of emittance to initial emittance.

A filamentation process can be seen in the phase-space where the phase-space ellipse becomes distorted into a spiral-like structure. As the particles are expelled from the core they lead to a filamented core or produce new tails. The new tails are continuously pushed out from the core, but always stay inside the original tail. This phenomenon provides a rough description of the halo formation. When a significant portion of particles is expelled the particles remaining inside the core see a reduced charge, which results in a new set of expelled particles that follow separatrices in the phase space that are closer to the core. For higher space charge the beam undergoes more severe density redistribution and the detailed halo structure becomes more diffuse. The result is a "peanut-shape" in phase space without an obvious filamentation structure.

Now we modified the IFMIF SRF-Linac tuning to avoid the *4th*-order coupling resonance $2\nu_z - 2\nu_x \approx 0$ centered at the tune ratio $\nu_z/\nu_x = 1$. The strength of solenoid magnetic field and the cavity electric field are modified. In Fig. 5 we plot the new tune footprint on the Hofmann charts for the emittance ratio $\epsilon_z/\epsilon_x = 1.5$. Note that the

ISBN 978-3-95450-115-1

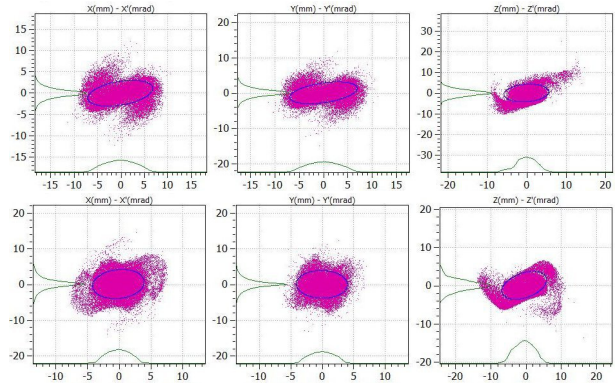

Figure 4: Phase space of halo particles $(x, x^{'})$, $(y, y^{'})$ and $(z, z^{'})$, respectively. Above : position $z = 3.9707$. Below : position $z = 10.8362$.

tune footprint now avoids the resonance $2\nu_z - 2\nu_x \approx 0$. It intercepts the resonance $\nu_z - 2\nu_x \approx 0$. Yet a part of tune footprint overlaps with the "sea of instability".

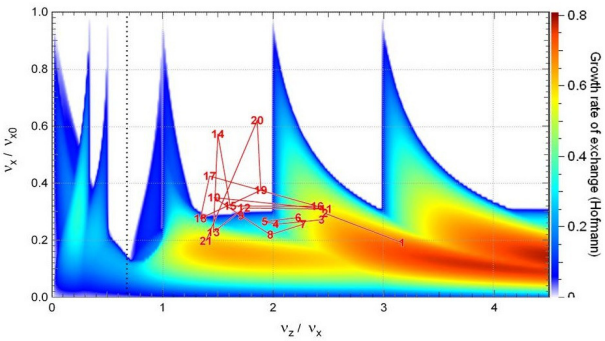

Figure 5: Stability chart for $\epsilon_z/\epsilon_x = 1.5$. Modified IFMIF SRF-Linac design. Dashed line indicate equipartition tune ratio.

The normalized emittance variation for the modified IFMIF SRF-Linac design is shown in Fig. 6. There is a weak emittance coupling between longitudinal and transverse planes caused by the "sea of instability". The growth of the rms emittance is showed by variation of ratio of emittance to initial emittance in Fig 6. The "peanut-shape" and filamentation structure are always present in the phase space, see Fig 7.

CONCLUSIONS

We have identified the modes of collective space charge density oscillations that are responsible for the transfer and growth of emittance in the IFMIF SRF-Linac. We found the space-charge resonances that are responsible for emittance coupling. The parametric resonances and filamentation processes were identified in phase space. They are responsible for emittance growth and halo formation. A detailed description of these phenomena is being prepared [6].

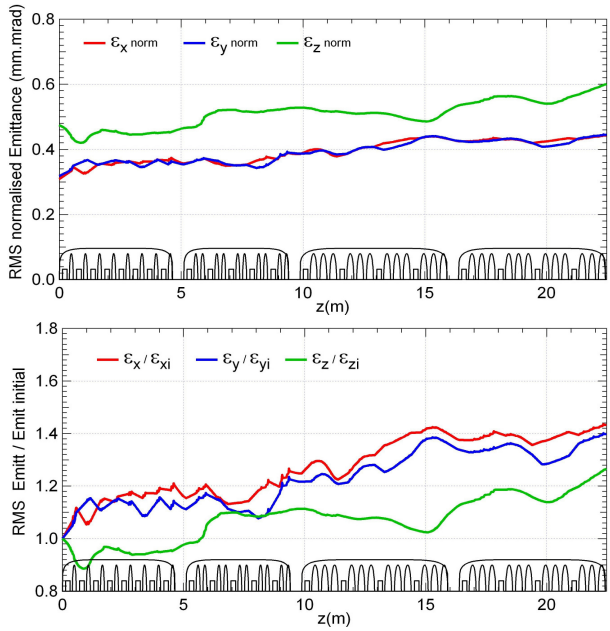

Figure 6: Above: normalised emittance along the modified IFMIF SRF-Linac design. Below : ratio of emittance to initial emittance.

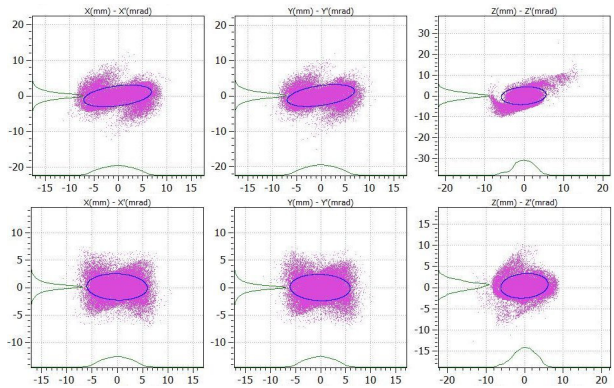

Figure 7: Phase space of halo particles $(x, x^{'})$, $(y, y^{'})$ and $(z, z^{'})$, respectively, for modified case. Above : position $z = 3.9707$. Below : position $z = 12.2596$.

REFERENCES

[1] A. Mosnier et al., Proc. of IPAC10, (2010). P.A.P. Nghiem et al., IFMIF-EVEDA Report : IFMIF-EVEDA-ASG-BD10-R006-A, (2010).

[2] I. Hofmann, Phys.Rev. E 57 (1998) 4713. I. Hofmann et al., Phys. Rev. ST Accel. Beams 6 (2003) 024202. G. Franchetti et al., Phys. Rev. Lett. 88 (2002) 254802. Ji Qiang et al., Phys. Rev. Lett. 92 (2004) 174801.

[3] R.L. Gluckstern, Phys. Rev. Lett. 73 (1994) 1247. J. Qiang, D. Ryne, Phys. Rev. ST Accel. Beams 3 (2000) 064201. R.L. Gluckstern et al., Phys. Rev. E 58 (1998) 4977. A.V. Fedotov et al. Phys. Rev. ST Accel. Beams 2 (1999) 014201.

[4] http://irfu.cea.fr/Sacm/logiciels/index.php.

[5] W. Simeoni Jr. et al., Proc. of IPAC11, (2011).

[6] W. Simeoni Jr. et al., Article in preparation.

ISBN 978-3-95450-115-1